Results in Physics 7 (2017) 644–650

Contents lists available at ScienceDirect

Results in Physics

journal homepage: www.journals.elsevier.com/results-in-physics

Development of reinforced in-situ anti-corrosion and wear $Zn\text{-}TiO_2/ZnTiB_2$ coatings on mild steel

O.S.I. Fayomi [a,b,*], A.P.I. Popoola [a], L.R. Kanyane [a], T. Monyai [a]

[a] Department of Chemical, Metallurgical & Materials Engineering, Tshwane University of Technology, P.M.B. X680, Pretoria, South Africa
[b] Department of Mechanical Engineering, Covenant University, P.M.B. 1023, Canaan Land, Ota, Nigeria

ARTICLE INFO

Article history:
Received 8 November 2016
Received in revised form 13 January 2017
Accepted 14 January 2017
Available online 18 January 2017

Keywords:
$Zn\text{-}TiO_2/Zn\text{-}TiB_2$
Solanum
Strengthening
Wear
Microhardness

ABSTRACT

The development of reinforced composite coating has resulted into advanced engineering application because of the exceptional properties and increase service life. In this study, we investigated the effect of Solanum tuberosum (ST) as additive to $Zn\text{-}TiO_2/Zn\text{-}TiB_2$ sulphate bath coating by co-deposition route on mild steel. The structural characteristics and surface profile of the produced coating were examined using scanning electron microscope coupled with energy dispersive spectroscopy (SEM/EDS) and PosiTector (SPG) respectively. The anti-corrosion resistance activities of the deposited coatings were evaluated on a 101 AUTOLAB potentiostat/galvanostat device in a 3.65 wt% NaCl. The wear characteristics of the $Zn\text{-}TiO_2/TiB_2$ composite coatings were examined on a dry abrasive MTR-300 test rig. The thermal stability of the produced coatings was studied in an isothermal furnace at 600 °C and further characterized using a high tech optical microscope. From the results, it was found that $Zn\text{-}TiO_2/Zn\text{-}TiB_2$ were compassed with needle like pattern and perhaps a compact and distinctive structure was found with $Zn\text{-}TiO_2/Zn\text{-}TiB_2/ST$ coatings. The microhardness deposited coatings increased with TiO_2 and TiB_2 interference in the plating bath, more significant improvement was noticed in the presence of natural bath-additive and the addition of ST lead to changes in the morphologies of the composite coatings. A massive decrease in corrosion and wear rate in all coatings produced as against the control sample was noticed. This was attributed to the dispersive strengthening activities of the embedded $TiO_2/TiB_2/ST$ additive on the bath formed.

Introduction

The excellent physical and mechanical properties of mild steel have made it widely used metal manufacturing engineering processes till date [1–3]. Meanwhile, it is true fact that the electrochemical resistance behaviour of mild steels in the presence of sulphide, chloride and moisture, with its stability at high temperatures are its shortfall [4–6]. In an attempt to enhance this stringent catastrophe of hostile condition, corrosion degradation and mechanical impunity, several reliable routes such as vapor deposition, hot dipping, electroless coating, cold spray has been used [7,8]. Surface modification methods to provide suitable protective protection against high temperature erosion and tribological fallout are necessary with the aim to have low cost products, less stress initiation, lower thickness to weight ratio [8].

Electrodeposition is a unique technological route for fabricating highly improved nanoparticulates coatings. It require less cost usage in production, quick deposition rate, low energy induced, ease to handle complex geometries, easy accesses to routine maintenance, control of internal and external operational system [9,10].

The impact of composite deposition of recent has been massive due to the novel properties possessed and its impact to engineering world. Composite co-deposition is a novel technology to obtain particle reinforced MMC or CMC in an attempt to obtain a matrix metal with organic or inorganic particle [11]. These composite coatings consist of matrix metals which are enhanced by second phase particulate thoroughly distributed within the metal matrix and thereby holding excellent wear resistance characteristics, good structural compatibility, improved corrosion and wear performance, stable thermal efficiency and reduced stress initiation [11,12].

Titanium oxide (TiO_2) has several applications in industrial and domestic fields due to its properties such as photo catalytic properties, good thermal stability, and excellent structural behaviour [12]. Titanium diboride (TiB_2) is a ceramic material with relatively

* Corresponding author at: Department of Chemical, Metallurgical & Materials Engineering, Tshwane University of Technology, P.M.B. X680, Pretoria, South Africa.
E-mail addresses: Ojosundayfayomi3@gmail.com (O.S.I. Fayomi), Popoolaapi@tut.ac.za (A.P.I. Popoola).

http://dx.doi.org/10.1016/j.rinp.2017.01.021
2211-3797/© 2017 Published by Elsevier B.V.

high strength and durability as characterized by the relatively high values of its melting point, hardness, strength to density ratio, and excellent wear resistance [9,12].

More importantly is the challenge of additive in controlling the bath framework for specific coatings. Several efforts by authors [13–15] showed that the preferred orientation in codeposited alloy is dependent on the deposition parameter and most especially the additives. It was affirmed that crystal growth are often inhibited by surface active additive. Glycerin, Thiourea, and others are reported as examples of additional inorganic and metallic ingredients that perform such role of improving properties of coatings [16,17]. Natural additives are said to better the morphology, reduce porosity and helps with good performance of coatings [13,18]. In this work, a detailed study of the nontoxic, cheap organic juice extract on the microstructural properties of Zn-TiO_2/TiB_2 and Zn-TiO_2/TiB_2/ST alloy is presented in an attempt to reduce undue structural stress initiation, improve corrosion properties and enhance mechanical characteristics.

Materials and methods

Material preparation

Mild steel samples (60 mm × 40 mm × 1 mm dimension) with the chemical composition shown in Table 1 were used as substrate and the anodes sheets used were 99.9% zinc with dimension of 30 mm × 20 mm × 1 mm. Chemicals used were Analar grade. Electrodeposition bath solution was prepared using distilled water. Subsequently the surface preparation of the mild steel sample was prepared with different grades of grinding paper in the order of 60 μm, 120 μm, 400 μm, 800 μm and 1600 μm to provide mirror-like free scale defects which are in par with previous study by [19]. Samples were activated by dipping in 1 mol HCl solution for 15 s followed by rinsing in distilled water.

Solanum tuberosum fluid extraction

Solanum tuberosum tuber of equivalent weight of 15 g were selected, peeled, washed and sectioned into smaller pieces. Then the smaller pieces were squeezed into deionized water to remove the fluid. The mined juice was stored in clean bottles and refrigerated. The Solanum tuberosum tuber used was shopped from Pretoria, South Africa. The molecular structure of Solanum tuberosum is presented in Fig. 1.

Preparation of coating formation

The prepared sample was dipped in a solution containing dissolved bath constituents which was heated for 1hour and simultaneously stirred at 150 rpm to obtain homogenous solution. Cathode and Anodes were connected to the D.C. power supply through a rectifier. Electrodeposition was carried out with applied voltage of 3 V for 20 min. With the depth of dipping and distance from cathode to anode kept constant. Immediately after the plating, rinsing was done in distilled water and samples were air-dried. The bath composition and process parameters are shown in Table 2.

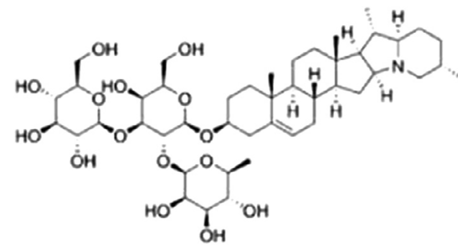

Fig. 1. Molecular structure of Solanum tuberosum.

Table 2
Bath Composition of Zn-TiO_2/TiB2/Solanum and Operating Condition.

Composition	Mass Concentration (g/L)
$ZnSO_4$	70
TiO_2	15
TiB_2	15
Solanum tuberosum	10(ml)
Boric Acid	10
$NaSO_4$	20
Glycine	10
Thiourea	10
pH	4.2
Voltage	3 V
Time	20 min
Temp.	40 °C

Table 3
Summarized data of Zn-TiO_2/TiB_2/Solanum plated samples for constant plating time at various current.

Sample order	Time of deposition (min)	Potential (V)	Current density (A/cm^2)
As received	–	–	–
Zn-TiO_2	20	3	3.5
Zn-TiO_2- Solanum	20	3	3.5
Zn-TiB_2	20	3	3.5
Zn-TiB_2-Solanaum	20	3	3.5

The experimental fabricated systems obtained for Zn-TiO_2/TiB_2/Solanum electro-deposition are showed in Table 3. The deposition voltage and time were kept constant.

Morphological studies

The structural evolution was characterized on Olympus BX51M Optical Microscope (OM) and Joel JSM6510 Scanning Electron microscopy (SEM) equipped with Energy Dispersive Spectroscopy (EDS).

Microhardness characterization and abrasive wear studies

Micro-hardness study of the produced coatings was examined using diamond pyramid indenter emco microhardness tester with a build in camera. A load of 10 g for a period of 10 s was used for the hardness characteristics. The indentation was taken at 4 different measurement location within the surface interface after which an average was obtained. Additionally, Surface texture were also determined using Positector texture tester. The wear mass loss

Table 1
Spectrochemical Analysis of Mild steel Sample.

Element	C	Mn	Si	P	S	Al	Ni	Fe
Composition (%)	0.15	0.45	0.18	0.01	0.031	0.005	0.008	99.166

was determined using MTR-300 dry abrasion tester machine under dry medium conditions utilizing silica sand as wearing medium at the speed of 200 rev/min for 60 s. The initial mass of the coated sample were weighed before the test and the final mass loss were taken after the test. These values were used to calculate the% mass loss of coated alloys.

Corrosion study

μAUTOLAB Pontentiostat/Galvanostat was used to study the corrosion behaviour of as-received sample and that of the deposited coatings in 3.65 wt% NaCl environment. The polarization measurements were carried from a start potential of −1.5 to an end potential of +1.5 V at a scanning rate of 0.01 V/s.; saturated calomel electrode was used as a reference electrode and graphite served as a counter electrode. The deposited sample was the working electrode with an exposed surface area of 1 cm^2. The entire body of the specimen was exposed to the corrosion environment. Nova 1.8 software was used to extrapolate the progression of the corrosion activity obtained from Tafel plots.

Results and discussion

Microstructural studies

Figs. 2–3 showed the scanning electron micrographs and attached EDS of the deposited samples. In all, the co-deposited appearance of the coatings shows preferred adhesion and stable deposit. The micrograph of Zn-TiO_2-Solanum (Fig. 2a) and Zn-TiB_2-Solanum (Fig. 3a) shows a buildup dispersive grains and compact crystalline structure as compared with Zn-TiO_2 (Fig. 2b) and Zn-TiB_2 (Fig. 3b) coating which possess randomly clumped distribution of particulate. This implies that the nature of the orientation of deposited structure is a function of the deposited variable especially the concentration of weight fraction of the induced matrix composite. This result was in par with the work of [4]. One significant observation of external surface feature of deposited coating containing Solanum tuberosum is the reduce stress appearance and better adhesion bond between the coating and the substrate. Even though, there are little continuous heterogeneous in term of grain from the micrograph in the presence Solanum tuberosum there were no porosity, damages and cavities seen. In other word, the morphological change noticed is due to the presence of Solanum tuberosum as additive, reason been that surface active activities of the adsorbate may have been responsible for the surface conditioning and perfect precipitation of the coating observed. This accession was also attested to by [13]. The Zn-TiO_2 and Zn-TiB_2 coating does not contain any cracks appearance or traces as well however, the resulting structure could not be compare to the nature of deposited coating obtained from ST induced. This result was in par with the work of [20]. The energy dispersion spectrum (EDS analysis) was engaged to extrapolate the elemental composition of the deposited coatings (Figs 2–3). There is clear corroboration between the EDS of the coating with and without Solanum tuberosum on zinc based matrix results. Both Zn-TiO_2-Solanum and Zn-TiB_2-Solanum showed Zn, O, Ti, peaks. The existence of some primary Ti single in the vicinity of all deposited coatings confirmed the presence of TiO_2/TiB_2 in the bath. This result is in par with the work of [9,14].

Fig. 4 shows the surface profile (texture) of the coated samples using Positector gage. From the results, the coating texture of Zn-TiO_2/Zn-TiB_2 was rougher than that of Zn-TiO_2/TiB_2-Solanum. Thus, the addition of Solanum tuberosum to the plating bath as an additive have inhibiting characteristics of reducing the coating texture as seen from the results. Although this observation is not far fetch from the distinctive assertion by Monyai et al. [20] and

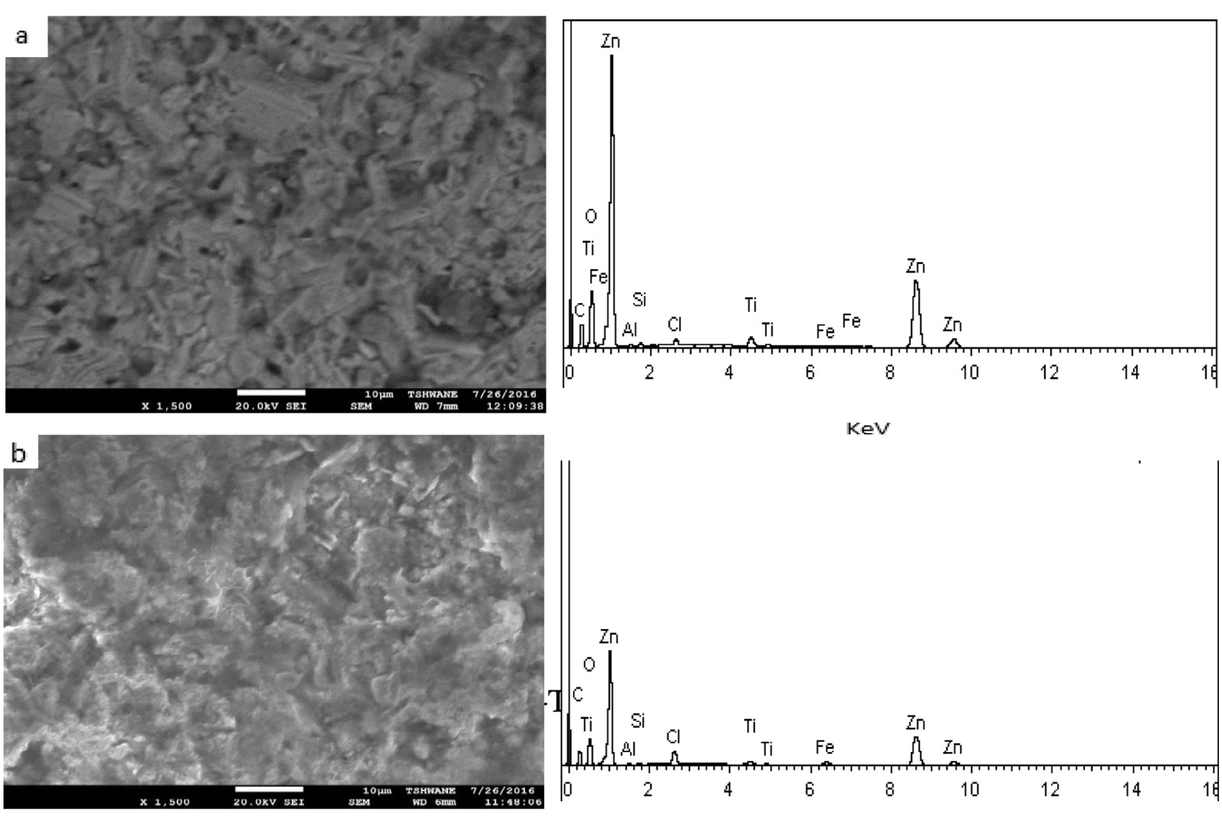

Fig. 2. SEM/EDS Micrographs a) Zn-TiO_2 b) Zn-TiO_2-Solanum.

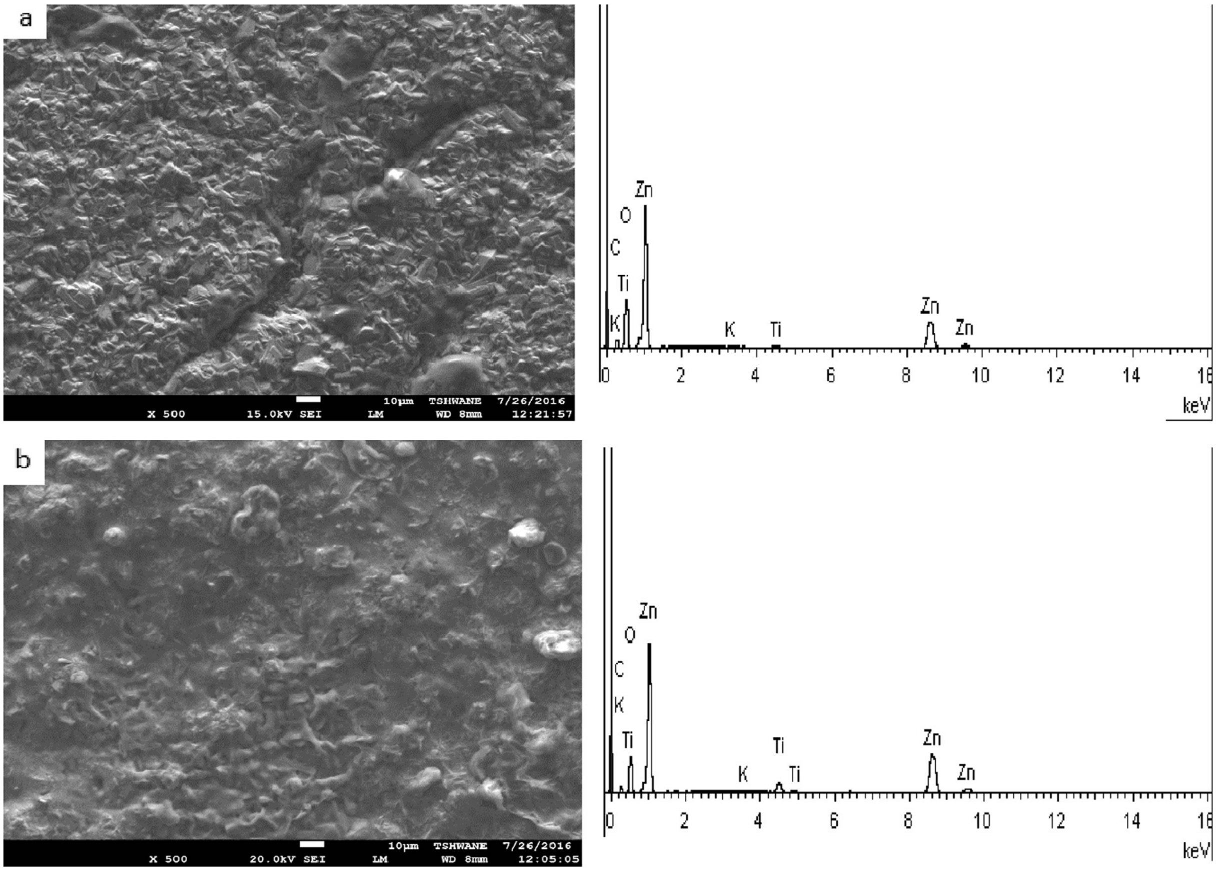

Fig. 3. SEM/EDS micrographs of a) Zn-TiB_2 b) Zn-TiB_2-Solanum.

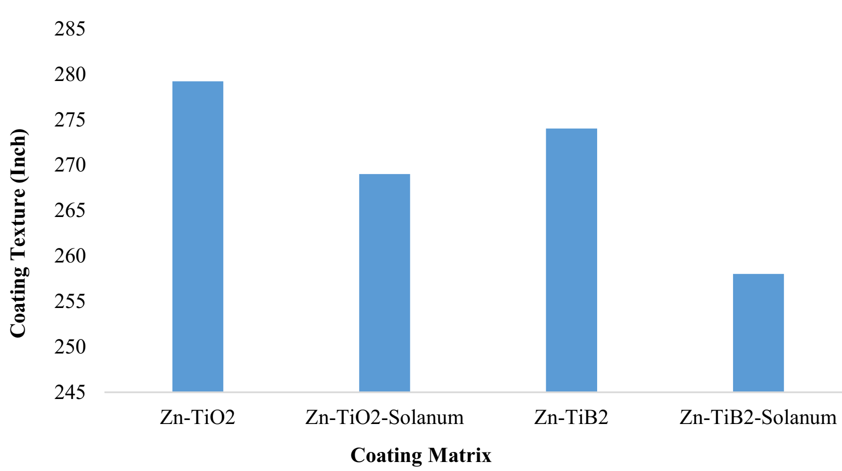

Fig. 4. Coating texture of Zn-TiO_2/TiB_2-Solanum coatings.

Saha [21] that solid particle often are surrounded by adsorbed ions, hence when the particulate reach the cathode surface it resulted into distinctive growth of metal matrix by coulomb forces. These observations by Saha [21] imply that TiO_2 and TiB_2 can affect growth of crystals at the cathode layer which is in par with the observed results but could not really put in consideration the influence of the surface active activity such as adsorbate that could suppress the possible reduction in the growing of crystals. Among the series of coating Zn-TiB_2 -solanum has excellent coating texture.

Wear and microhardness resistance properties of the deposited coatings

The wear study of Zn-TiO_2/Zn-TiB_2 and Zn-TiO_2/Zn-TiB_2-Solanum coatings was carried out. Fig. 5 shows the summarized progression of the volume mass loss of the uncoated and coated samples. It may be noted that there is considerably decrease in wear plastic deformation of all coated samples with or without ST as against the as-received substrate samples. Therefore, from the generated results, it shows that the addition of Solanum

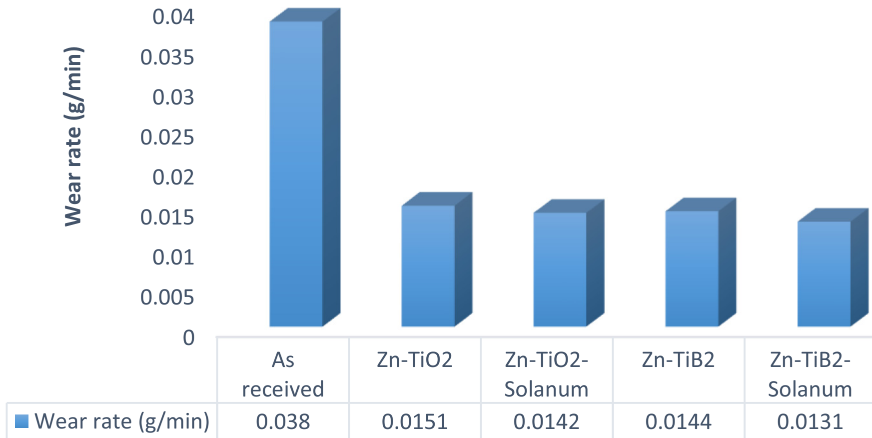

Fig. 5. Variation of wear rate of uncoated and coated samples.

tuberosum gives better improvement in anti-wear properties which is supported by result observed from [21]. The improved wear properties due to electrodeposited alloying with Zn- based metal is due to dispersion of *TiO_2/TiB_2*, and structural refinement by ST [9]. It is also needful to mention that in as-received sample, there is massive removal of materials from the warn surface with less observed on coated samples due to strong adhesive bonding between the substrate and the particles. There are no magical oxidations or generation of crack which might have resulted into severe wear out on the deposited coatings. Interestingly, it could be concluded that wear mechanism is a function of abrasive of the materials, structural bonding between the substrate and deposited coating and process parameter of the deposited coatings.

Fig. 6 shows the microhardness distribution of the electrodeposited Zn-TiO_2/Zn-TiB_2 and Zn-TiO_2/Zn-TiB_2-Solanum at constant current density before and after heat treatment. It was observed that Zn-TiB_2 and Zn-TiB_2-Solanum has good microhardness properties with 176 HV and 172 HV respectively before tempering, compare to Zn-TiO_2/Zn-TiO_2 –Solanum with 170 HV and 150.6 HV respectively. Meanwhile, there was a significant increase in microhardness behaviour from all coatings as against the as-received sample which is expected because of the development of surface–hardening properties exhibited from the deposited composite particulate. According to [1] and [2], the microhardness of the deposited samples often depends on many factors such as the composition of the plating bath, the effect of dispersion and the operating parameters. The highest hardness properties hence can be linked to the network of additives participating at the formation of the coatings [12]. It is noteworthy to mention that the content of Ti possesses high strengthening characteristics ordinarily and therefore its traces can pose a higher refined crystal size with boride, and oxide matrix as observed. Consequently this combine effect of oxide and boride in Ti matrix can be seen to provide the formation of hardness properties noticed. In observing the thermal stability, deposited sample were suggested to heat treatment at 600 °C. After the heat treatment, all deposited sample still retain their stability with less depreciation in hardness trend as observed in Fig 6. The recrystallization behaviour of the Zn-TiO_2/Zn-TiB_2-Solanum was presented in Fig. 7 with crystal evolution clearly showed with Zn-TiB_2-Solanum. There was no visible damages, crack and oxidation tendency noticed at the interface of the produced coatings.

Potentiodynamic polarization studies

The susceptibility of the fabricated coatings on mild steel to corrode in the 3.65% NaCl was investigated. Figs. 8–9 showed the polarization resistance and corrosion rate progression while Fig. 10 showed the morphological properties of the coated samples respectively. The results obtained from Fig. 8 indicated that there is increase in polarization potential with the addition of ST coated alloys both on Zn-TiO_2/Zn-TiB_2. The highest polarization reach (Rp) is 196.52 Ω for Zn-TiO_2-Solanum and lowest was found with Zn-TiB_2 with 115.01 Ω among the coating series. It is noteworthy

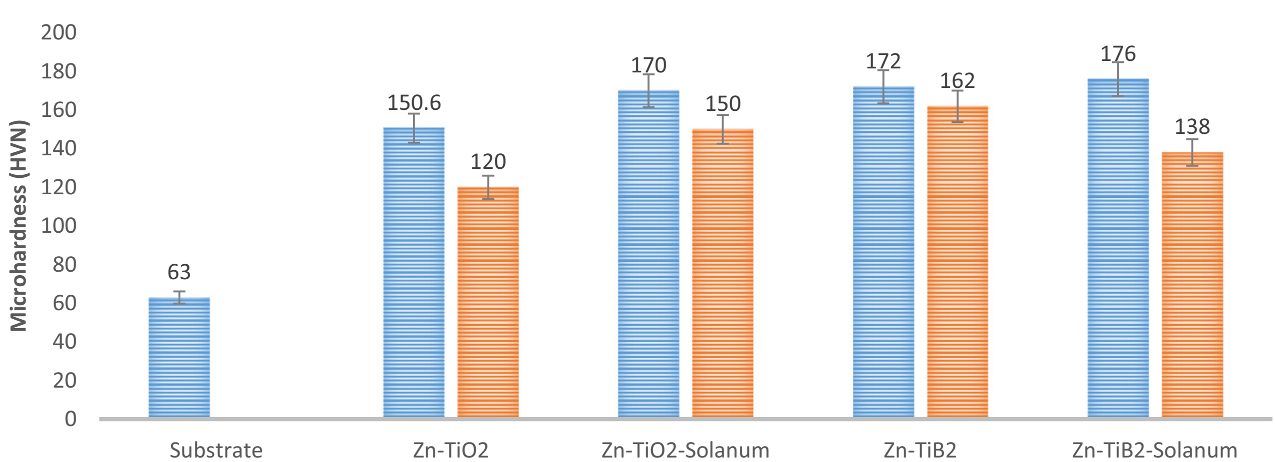

Fig. 6. Comparison of Microhardness of Zn-TiO_2/TiB_2-Solanum coating for heat treated and untreated samples.

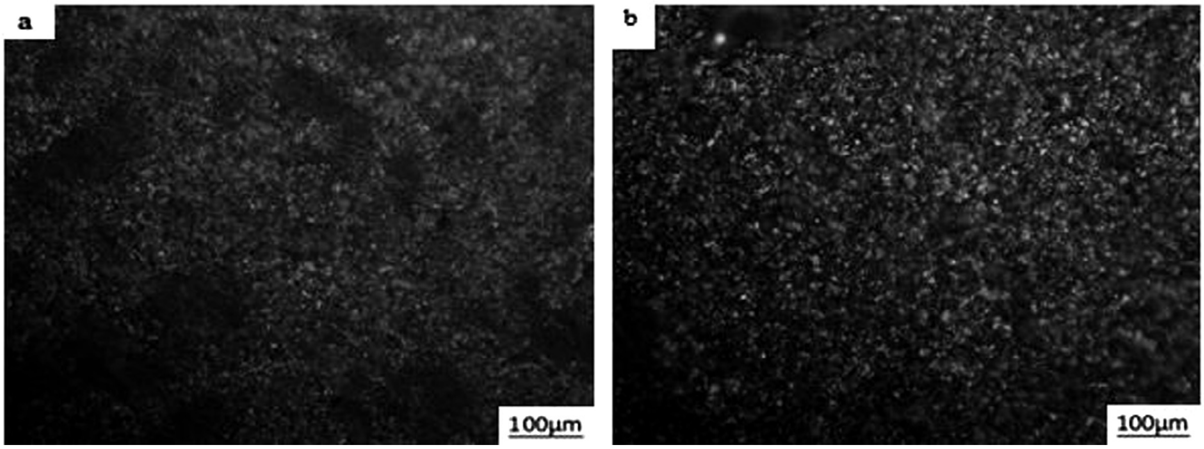

Fig. 7. Micrographs of the heat treated (600 °C) composite coatings on mild steel a) Zn-TiO_2-Solanum b) Zn-TiB_2-Solanum.

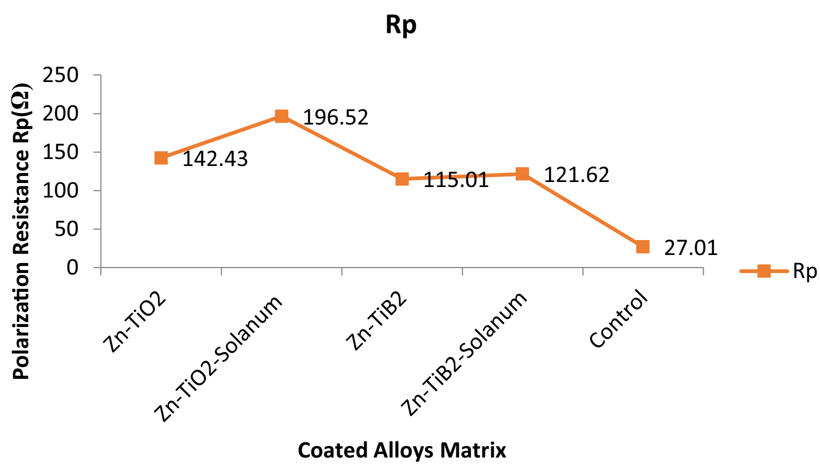

Fig. 8. Polarization Resistance Progression of coated alloys in 3.65% NaCl concentration at 298 K.

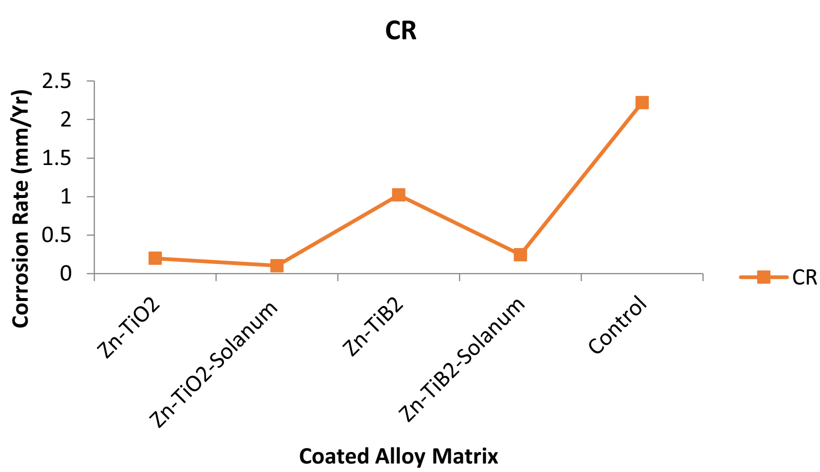

Fig. 9. Corrosion rate progression of coated alloys in 3.65% NaCl concentration at 298 K.

to mention that all coating on TiO_2 induced had massive improvement as against the TiB_2 support coatings, the reason might not been far fetch from the fact that the protective reactiveness of TiO_2 has superior protective prospect over TiB_2 with ceramics constituent. But, it is also good to mention that mild steel displayed lower polarization resistance due to lack of protective coverage.

From Fig. 9, it can be seen that the corrosion rate of the coatings follow same trend as polarization potential in the reverse order. The general decrease in corrosion rate as against the as-received sample is attributed to the excellent interfacial bonding and adhesion of the composites coating on the mild steel. The presence of ST decreases the corrosion propagation significantly as compare to

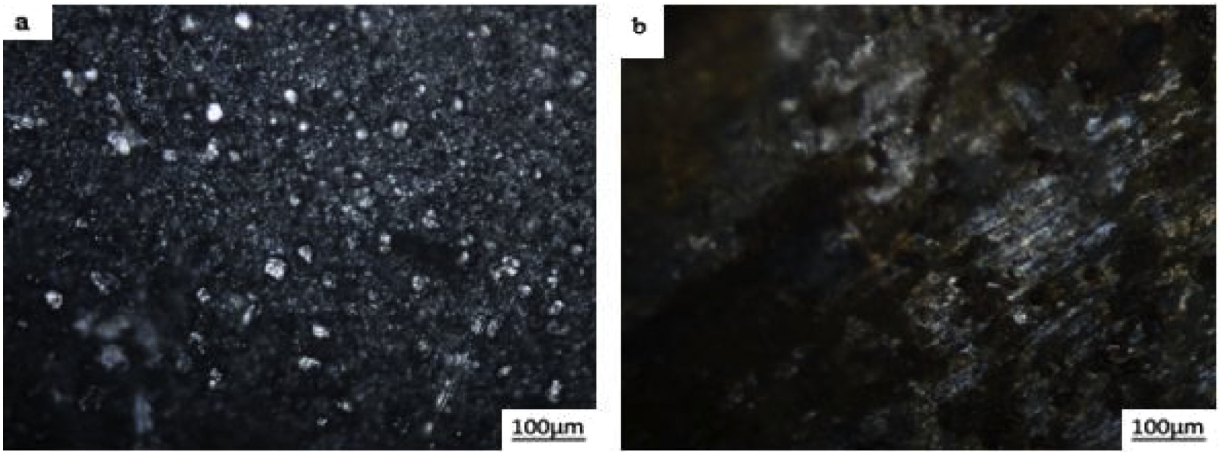

Fig. 10. Micrographs after corrosion in 3.65%NaCl a) Zn-TiO_2-Solanum b) Zn-TiB_2-Solanum.

other coating without ST interference, for instance corrosion rate of 0.1021 mm/year, 0.2455 mm/year and 2.221 mm/year were obtained for the Zn-TiO_2-ST/Zn-TiB_2-ST and control sample respectively. It is obvious that the coating on the mild steel conferred hedge on the active site that might thereby resist against salt attack which if not protected could have resulted to serious corrosion damage.

The optical images seen in Fig. 10a and b were taken to establish the interaction of the coating with mild steel surface. With Zn-TiO_2-ST have a better coating appearance with less corrosion product. Thus this observation implies that there are strong interfacial properties exhibited by the induced composite and additive lending to a hard phase behaviour that offer resistance to corrosion destruction. In the case of Zn-TiB_2-ST there is severe attack on the fabricated coating as showed in Fig 10b with pits and cavities, the damages noticed. This appeared that damaging act is as a result of contention between the TiB_2 and salt attack reason been that boride effect has little or no tendency of corrosion resistance characteristics.

Conclusions

- Zn-$TiO_{2,}$ Zn-$TiB_{2,}$ Zn-TiO_2-Solanum and Zn-TiB_2-Solanum were successfully co-deposited in the Zn based matrix by electrodeposition route with a current density of 3.5 A/dm^2 and applied potential of 3 V on mild steel substrate.
- A uniform distribution of Zn, Ti interference was observed in all cases as showed in the EDS pattern. The micrograph shows no evidence of porosity, crack or initiation of stress.
- Zn-TiO_2/Zn-TiO_2-Solanum matrix showed better corrosion resistance as compared to Zn-$TiB_{2,}$ Zn-TiB_2 –Solanum a clear cut evidence of influence of particle composition on fabricated coatings.
- The addition of Solanum tuberosum as additive to electrodeposition bath resulted improved structure with less coarse grain. The microhardness of the developed coatings increased to 176 HVN as compared to 63 HNV of mild steel substrate.
- Coatings with Solanum tuberosum addition also improved antiwear properties of the coatings. A decrease in plastic deformation and declamation was seen from 0.038 to 0.0131 g/min.

Acknowledgements

The financial supports from National Research Foundation (NRF) South Africa, the equipment support by Surface Engineering Research Centre (SERC), Tshwane University of Technology Pretoria South Africa are gratefully acknowledged.

References

[1] Popoola API, Fayomi OSI, Popoola OM. Int. J. Electrochem. Sci. 2012;7:4860–70.
[2] Fashu S, Gu CD, Zhang JL, Bai WQ, Wang XL, Tu JP. Surf. Int. Anal. 2015;47:403–12.
[3] Eliaz N, Venkatakrishna K, Chitharanjan A. Hegde Surf. Coat. Technol. 2010;205:1969–78.
[4] Fayomi OSI, Popoola API. Acta Metall. Sin. (English Letters) 2015;28:521–30.
[5] Fayomi OSI, Popoola API. Surf. Eng. Appl. Electrochem. 2015;51:76–84.
[6] Shibli SMA, Dilimon VS, Smitha P, Antony R. Manuf. Surf. Coat. Technol. 2006;200:4791–6.
[7] Kumar MKP, Venkatesha TV, Pavithra MK. Phys. Scr. 2011;84:035601.
[8] Munro RG. J. Res. Natl. Inst. Stand. Technol. 2000;105:709–20.
[9] Fayomi OSI, Aigbodion VS, Popoola API. J. Fail. Anal. Prev. 2015;15:54–64.
[10] Fayomi OSI, Joseph OO, Mubiayi MP, Durodola BM, Gabriel O. Egypt. J. Basic Appl. Sci. 2015;3:1–9.
[11] Fayomi OSI, Popoola API. Int. J. Electrochem. Sci. 2012;7:6555–70.
[12] Fayomi OSI, Popoola API, Aigbodion VS. J. Alloy Compd. 2014;617:455–63.
[13] Loto CA, Olofinjana A, Popoola API. Int. J. Electrochem. Sci. 2012;7:9795–811.
[14] Tuaweri J, Gumus R. Int. J. Mater. Sci. Appl. 2013;6:221–7.
[15] Fayomi OSI, Popoola API. Res. Chem. Intermed. 2015;41:2393–405.
[16] Amuda MOH, Subair W, Obitayo OW. Int. J. Eng. Res. Afr. 2009;2:31–9.
[17] Malatji N, Popoola API, Fayomi OSI, Loto CA. Int. J. Adv. Manuf. Technol. 2016;82:1335–41.
[18] Shamsolhodaei A, Rahmani H, Rastegari S. Surf. Eng. 2013;29:695–9.
[19] Fayomi OSI, Abdulwahab M, Popoola API. J. Ovonic Res. 2013;9:123–32.
[20] Monyai T, Fayomi OSI, Popoola API. Portuga Electrochem Acta 2016;34:355–63.
[21] Saha RK, Khan TI. Surf. Coat. Technol. 2010;205:890–5.